Journal of Digital Imaging (2018) 31:646–654
https://doi.org/10.1007/s10278-018-0083-x

Andriod Device-Based Cervical Cancer Screening for Resource-Poor Settings

Vidya Kudva[1,2] · Keerthana Prasad[1] · Shyamala Guruvare[3]

Published online: 18 May 2018

Abstract
Visual inspection with acetic acid (VIA) is an effective, affordable and simple test for cervical cancer screening in resource-poor settings. But considerable expertise is needed to differentiate cancerous lesions from normal lesions, which is lacking in developing countries. Many studies have attempted automation of cervical cancer detection from cervix images acquired during the VIA process. These studies used images acquired through colposcopy or cervicography. However, colposcopy is expensive and hence is not feasible as a screening tool in resource-poor settings. Cervicography uses a digital camera to acquire cervix images which are subsequently sent to experts for evaluation. Hence, cervicography does not provide a real-time decision of whether the cervix is normal or not, during the VIA examination. In case the cervix is found to be abnormal, the patient may be referred to a hospital for further evaluation using Pap smear and/or biopsy. An android device with an inbuilt app to acquire images and provide instant results would be an obvious choice in resource-poor settings. In this paper, we propose an algorithm for analysis of cervix images acquired using an android device, which can be used for the development of decision support system to provide instant decision during cervical cancer screening. This algorithm offers an accuracy of 97.94%, a sensitivity of 99.05% and specificity of 97.16%.

Keywords Automated cervical cancer detection · Android device-based cervical cancer screening · Low-resource cervical cancer screening

Introduction

Cervical cancer is a slowly progressing disease and is amenable for screening and early detection. In spite of this, it has been ranked second among cancers affecting the women globally [1–3]. Some of the commonly used screening tests for early detection of cervical cancer are Pap smear, HPV-DNA and visual inspection with acetic acid (VIA). Pap smear is the most commonly used method for cervical cancer screening. It depends on availability of laboratory facility and medical experts for smear preparation and analysis, which is lacking in developing countries. VIA evaluates the cervix for acetowhite (AW) regions which are formed when precancerous lesions combine with acetic acid. It does not depend on well-established laboratory facility and hence is a cost-effective test. It is a simple test as it is based on visual examination of the cervix after the application of acetic acid. Thus, it is well suited for screening in developing countries [2–5]. Cervix images with acetowhite lesions are designated as VIA positive and images without acetowhite lesion as VIA negative. A few images of VIA-positive category are shown in Fig. 1. Precancerous lesions have turned white in Fig. 1b which is marked as AW.

Figure 2 shows few cervix images of VIA-negative category. Acetowhite regions are not present after the application of acetic acid as in Fig. 2b.

However, considerable expertise is needed to evaluate the acetowhite regions for decision-making. Though VIA is a suitable test for low-resource settings as far as the simplicity of the test is considered, it requires skilled personnel for the evaluation of the acetowhite regions. Depending on the skills

✉ Keerthana Prasad
keerthana.prasad@manipal.edu

Vidya Kudva
vidyakamathkudva@gmail.com

Shyamala Guruvare
shyamala.g@manipal.edu

[1] School of Information Sciences, Manipal Academy of Higher Education, Manipal, Karnataka 576104, India

[2] NMAMIT, Nitte 574110, India

[3] Department of Obstetrics and Gynecology, Kasturba Medical College, Manipal, Karnataka 576104, India

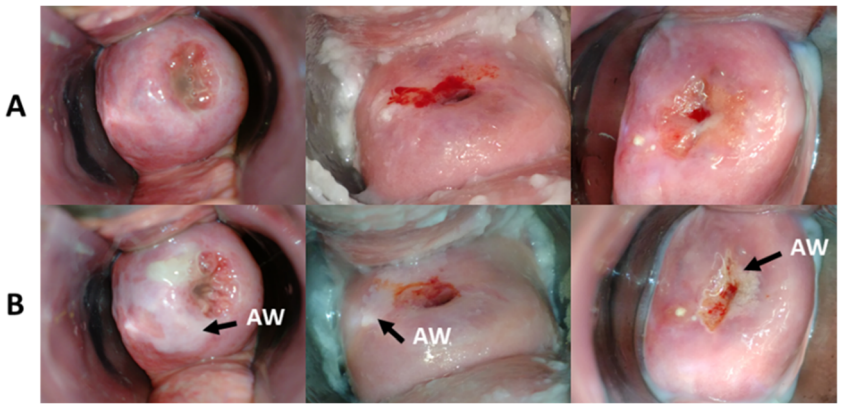

Fig. 1 VIA-positive images. The cervix images **a** before application of acetic acid and **b** after application of acetic acid

of the ones who perform the test, accuracy of VIA varies widely, with significantly higher sensitivity and specificity when observed by physicians than by nurses [6]. An automated system for cervix image analysis might be able to overcome this problem, providing objective and repeatable evaluations. Advances in digital imaging and image processing have facilitated the acquisition of good-quality cervix images during the VIA procedure. At present, digital images of the cervix are acquired using a digital camera or a digital colposcope. Acquisition of cervix images using the digital camera and subsequent analysis of the images by skilled personnel is called cervicography. Since images acquired can be stored and sent over the Internet, it enables remote diagnosis. Digital colposcopy facilitates the acquisition of high-magnification cervix images. However, it is expensive and hence is not feasible for screening in resource-poor settings. An android device with an inbuilt app to acquire images and provide instant results would be an obvious choice in resource-poor settings.

Our overall goal is to develop a decision support system for cervical cancer screening which facilitates acquisition and processing of images with an inbuilt image processing algorithm. Such a system would be useful to augment the capability of a lay health worker performing the VIA examination to offer instant decision whether the individual requires further evaluation or not. In this paper, we present the development of image processing algorithm for classification of cervix images into VIA positive or negative.

Related Work

Image processing algorithms have been developed to process images acquired through colposcopy and cervicography. In both the cases, image processing algorithm covers various tasks such as specular reflection (SR) removal [7–9]; detection of anatomical landmarks such as os, columnar epithelium (CE) and squamous epithelium (SE) [10–12]; region of interest (ROI) detection [10, 13, 14]; acetowhite detection [15–21]; and texture detection [22–26]. Image processing algorithms developed for analysis of colposcopic images aimed at assisting the physicians to build their colposcopic diagnosis and/or to automatically identify the region for biopsy on the cervix region. Algorithms developed for analysis of cervicography images identified various landmarks for analysis. They also studied the feasibility of computerised cervical cancer screening. A few researchers [27–30] evaluated the feasibility of using commercially available smartphones for acquisition of cervix images during VIA in resource-poor settings and remote diagnosis by experts using these cervix images. But these studies were limited to interobserver

Fig. 2 VIA-negative images. The cervix images **a** before application of acetic acid and **b** after application of acetic acid

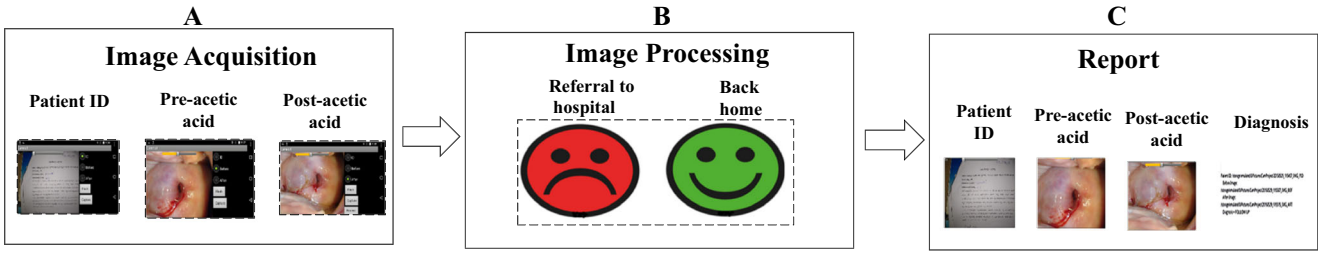

Fig. 3 Decision support system for cervical cancer screening

variability study. Automated analysis of images acquired using commercially available android devices is not reported to the best of our knowledge.

Methodology

The block diagram of the proposed decision support system is shown in Fig. 3.

The proposed decision support system consists of three modules, namely image acquisition (Fig. 3, block A), image processing (Fig. 3, block B) and generation of report (Fig. 3, block C). In this paper, we present the details of image acquisition and image processing.

Image Acquisition

A schematic of the image acquisition setup is shown in Fig.4.

During VIA examination (Fig. 4a), the health care professional inserts a speculum as shown in Fig. 4b into the vagina of the patient to view the cervix and acquires the image using an android device docked on to the speculum (as shown in Fig. 4c, d). We acquired the images through the camera of android device with 13MP camera under uniform lighting condition with dual tone LED flash. An android app was developed for image acquisition which had the options of acquiring the images of patient IDs, cervix image before application of acetic acid and after application of acetic acid. Images were acquired in screening programmes at the health centres, conducted by the Kasturba Medical College, Manipal, Karnataka, India. Married women above 25 years of age were considered for the study. Informed consent was obtained from the women participating in the study. A medical expert in the field of cervical cancer screening manually evaluated all the acquired images, annotated the region of interest and provided the gold standard whether images were VIA positive or negative. A total of 102 cervix images, 42 VIA positive and 60 VIA negative, were considered for this study.

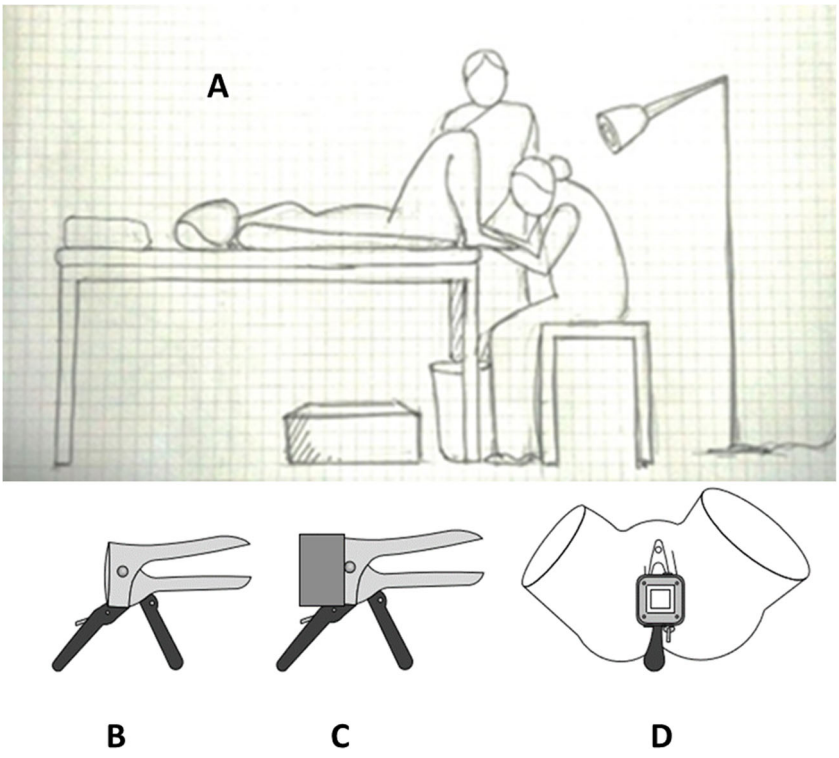

Fig. 4 Image acquisition setup. **a** VIA examination setup **b** Speculum **c** Android device docked on to speculum **d** Speculum with device docked in vagina

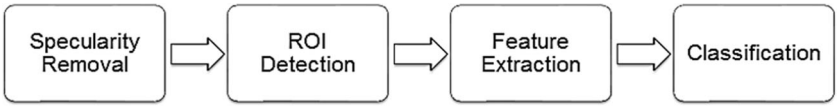

Fig. 5 Block diagram for cervix image analysis

Image Processing

An image processing algorithm was built using MATLAB R2017a. It consists of four stages, namely SR removal, ROI detection, feature extraction and classification as shown in Fig. 5.

Specular Reflection Removal

Specular reflections are bright white regions on the cervix image caused due to reflection of light from wet surface of the cervix. These regions have high intensity, contrast and saturation values. A combination of the saturation (S) component of hue, saturation and value (HSV) color space representation, the green component (G) of original image and the lightness (L) component of CIE-Lab color space representation highlighted the SR regions in a distinct manner. All these components were normalised to have values between 0 and 1. A feature image F was obtained by using the following equation:

$$F = ((1-S) \times G \times L)^3 \quad (1)$$

Different steps involved in SR detection are depicted in Fig. 6.

The feature image was filtered using a standard deviation filter of size 3. Output of the filter was normalised to have values between 0 and 1. It was observed that the filter output value was close to 1 at the contours of SR regions. Hence, a value of 0.9 was used to the threshold the output of the filter. The thresholded image was filled and subsequently dilated using a disk-shaped structuring element of size 2. Each pixel in the SR region was assigned the mean color of its 5 × 5 non-zero neighbours.

ROI Detection

We use a method explained in [31] for ROI detection. Different stages used by this method for ROI detection in cervix images are shown in Fig. 7.

Red component of color image was filtered using zero mean filters with different directions and widths. Four different filter orientations 0°, 45°, 90° and 135° and three different filter widths 5, 6 and 7 were used which resulted in a total of 12 filters. Each of these filters highlighted curvatures present in a particular direction. The final image was obtained by taking the maximum of the corresponding pixel values of 12 images. The final image which is denoted as the curvature image in the paper highlights the curvatures in all four directions. The curvature image was thresholded to get a binary image. The threshold value was selected by taking the average of gray levels, whose pixel count is greater than 95% of the total number of pixels in the curvature image. This threshold value was selected from observation that most of the pixels in the output of filter were towards white and only few were towards black. The binary image was filled and the biggest area was selected as the coarse cervix region as shown in Fig. 9e. In the next step, all the points on the boundary of the biggest area were extracted. An ellipse which best fits these extracted points was estimated as in Fig. 9f and used as a mask for performing the logical OR operation with the coarse cervix region as in Fig. 9g. This step was required to manage appropriate selection of the cervix region in the cases of varied presentations of os. This step was followed by morphological operations to remove vaginal walls in case it has been selected as part of the cervix region.

Feature Extraction

Color is a more significant information for finding acetowhite lesions. Further, AW textures play an important role in grading acetowhite lesions [32]. We considered both color and texture features for image classification. Color is represented using eight features: mean and standard deviation of red (R), green (G) and blue (B) components of original image and value (V) component of HSV color space representation. We considered five types of texture features. First was Spatial Gray Level Dependence Matrix (SGLDM)-based features [33]. SGLDM was constructed by estimating second-order conditional probability density $P(i, j, d, \theta)$, that is, probability of moving from gray level i to gray level j, for a distance d between pixels and the direction θ. Four different directions $\theta = 0^\circ, 90^\circ, 135^\circ$ and 45° were used. A total of 26 features were extracted with $d = 1$. The second type

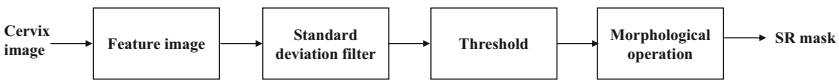

Fig. 6 Block diagram of SR detection algorithm

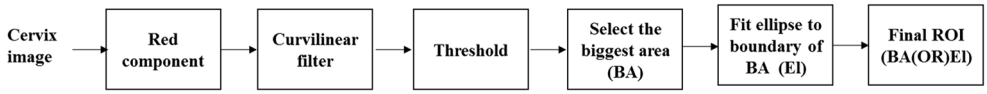

Fig. 7 Block diagram of ROI detection algorithm

of texture features was derived from Neighbourhood Gray-Tone Difference Matrix (NGTDM) [34]. A total of five features, namely coarseness, contrast, busyness, complexity and texture strength, were extracted. The third category of texture features was based on Neighbouring Gray Level Dependence Matrix (NGLDM) [35]. A total of five features were extracted from NGLDM. The fourth group contained 40 features extracted from wavelet coefficients. The green component of the original image was decomposed into four levels using wavelet decomposition. Mean and standard deviation of approximation coefficients at the fourth level were used as a feature set. The fifth group of texture features was derived from the local binary pattern (LBP) of image [36]. The fifth group had a total of 10 features. All 94 features extracted were normalised to have a zero mean and standard deviation of 1. Feature selection was used to reduce the number of features and to improve the classifier performance. The feature selection method based on the random subset feature selection (RSFS) [37] algorithm was used. In this method, a set of relevant features were found by choosing random subset of features from the full set of features repetitively and subsequently classifying the data with a classifier using these feature subsets. Relevance of each feature in the subset used during an iteration was adjusted based on the performance of the classifier. With increased number of iterations, the quality of the final feature set improves. Thus, the average relevance of each feature gets evaluated with respect to other feature subsets. Pseudo code for feature subset selection is shown in Algorithm 1.

This RSFS method has been adapted from Jouni et al. [37]. In this study, they used k-nearest neighbourhood classifier, unweighted average recall (UAR) as the criterion function and n was selected using the formula $\sqrt{\text{Cardinality}(F)}$. A threshold value of $\delta = 0.99$ was selected. In the proposed method, we used two classifiers as explained in the "Classification" section. Feature relevance was updated based on correct classification and misclassification. Mathematically, feature relevance updation is given by

$$r_j^{'} = r_j + c \tag{2}$$

Algorithm 1 Feature subset selection for a given classifier

Inputs: Full feature set F, number of iterations i, desired criterion function, classifier

Output: Best feature subset S for given classifier

1. *Randomly pick a subset* S_i *of* n *features from the full set* F
2. *Perform classification on the data set using subset* S_i
3. *Measure the value of the criterion function* c_i
4. *Update the feature relevance* r_j *by replacing it with* $r_j' = r_j +$ *criterion function*
5. *Repeat steps* 1 *to* 4 *until the criterion is met*
6. *Select* S *as all features satisfying the condition* $p(r_j > r_{rand}) \geq \delta$, *where,* r_{rand} *is the relevance of nonuseful features and* δ *is threshold value*

where criterion function c is given by $c = \frac{N_c}{N_c + N_{mc}}$, where N_c is the total number of correct classification and N_{mc} is

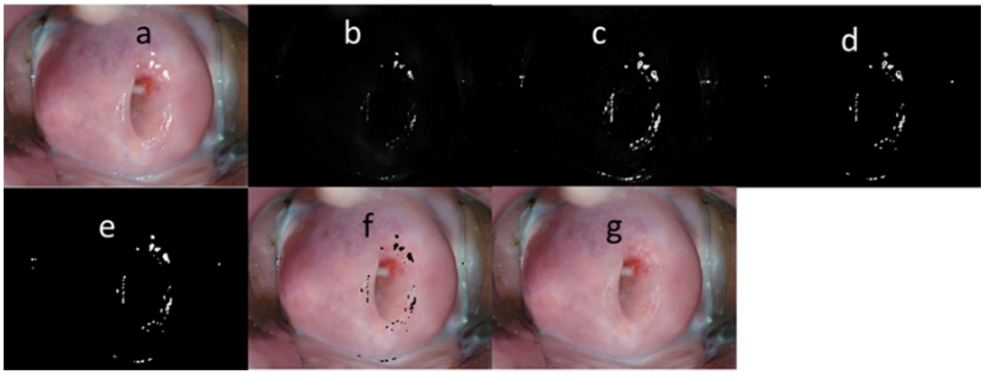

Fig. 8 SR detection using the standard deviation filter. **a** Cervix image. **b** Feature image. **c** Standard deviation filter output. **d** Thresholded image. **e** SR mask. **f** SR regions highlighted on the original image. **g** SR-removed image

the total misclassifications. Cardinality of F in the present case is 94. Hence, number n was selected as 10. The threshold value of $\delta = 0.99$ was used.

Classification

We used support vector machine (SVM) and decision tree (DT) classifiers [38] for classification of cervix images. The SVM classifier makes use of hyperplane to segregate the classes. SVM can also be used to segregate nonlinearly separable data using nonlinear kernels. We used SVM as a binary classifier to classify cervix images as VIA positive or negative. A DT classifier is constructed by finding the attribute with the highest entropy at each level. Tree pruning is used to overcome the problem of over fitting. We used DT as a binary classifier. Accuracy of each classifier was evaluated using k-fold and leave-one-out cross-validation. Three parameters, namely accuracy, sensitivity and specificity, were used to evaluate the performance of the classifiers.

Results

Cervix images were pre-processed to remove specular reflections and to identify the cervix region. Results of specular reflection removal algorithm are shown in Fig. 8.

Results of ROI detection are shown in Fig. 9.

We implemented ROI detection as explained in the "ROI Detection" section, extracted cervix mask and computed the metrics, namely dice metric, sensitivity metric, false positive metric and Hausdorff distance. Average values of these metrics were 0.904, 0.968, 0.181 and 104, respectively. Detected ROI is marked on the original image as shown in Fig. 9i. Black contour indicates the detected ROI using the proposed algorithm and white contour indicates the ROI annotated by the expert.

In the next step, color and five types of texture features (SGLDM, NGTDM, NGLDM, wavelet and LBP) were extracted. A feature selection method based on RSFS was used with SVM and DT classifiers. Performance of SVM and DT classifier for k-fold cross-validation is tabulated in Table 1.

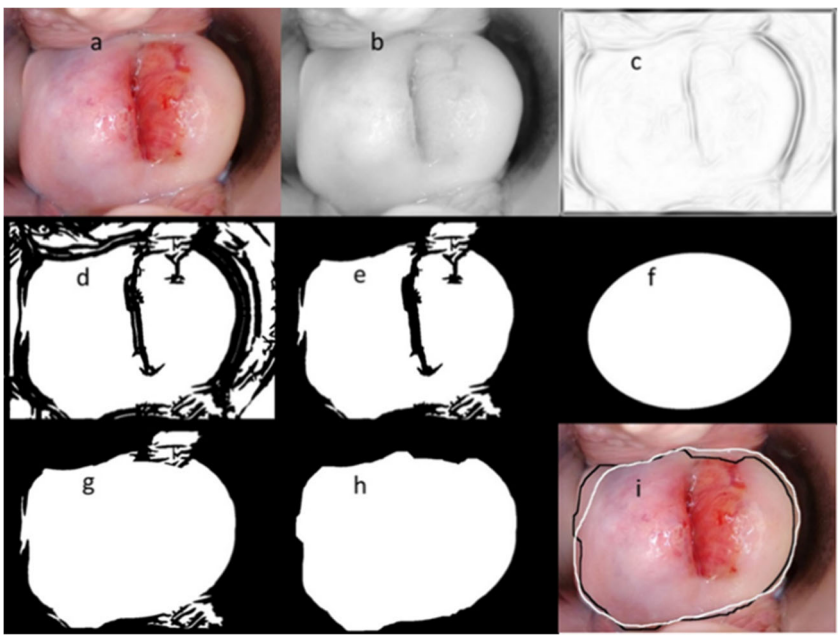

Fig. 9 Cervix region detection. **a** Cervix image. **b** Red component. **c** Curvature image. **d** Thresholding and filling. **e** Biggest area. **f** Ellipse mask. **g** Logical ORing (**e** and **f**). **h** Final ROI mask after morphological operation. **i** Detected ROI on the original image

Table 1 Performance of classifiers for *k*-fold cross-validation

k	SVM classifier			DT classifier		
	Acc. (%)	Sens. (%)	Spec. (%)	Acc. (%)	Sens. (%)	Spec. (%)
10	64.61	64.29	64.83	68.85	57.45	76.8
20	75.7	72.59	77.86	73.56	61.48	82.02
30	80.24	77.71	81.99	82.53	73.84	88.6
40	83.07	77.98	86.62	86.47	81.43	90
50	88.75	87.55	89.59	88.41	82.36	92.64
60	90.91	94.24	88.58	91.14	87.35	93.78
70	93.31	94.74	92.31	93.1	92.35	93.63
80	95.59	96.91	94.67	93.43	93.1	93.67
90	97.94	99.05	97.16	95.57	95.95	95.29
100	97.45	98.1	96.99	94.61	91.19	97

Acc. accuracy, *Sens.* sensitivity, *Spec.* specificity

Average values of various parameters over 10 iterations are tabulated.

A graph of variation in sensitivity of two classifiers as a function of folds (*k*) is shown in Fig. 10.

The average performance of SVM and DT classifiers over 10 iterations with RSFS feature selection and leave-one-out cross-validation is tabulated in Table 2.

Performance of the SVM classifier for $k = 90$ over 10 iterations is shown in Fig. 11.

Discussion

An image analysis algorithm for classification of cervix images was proposed. Performance of classification using SVM and decision tree classifiers was demonstrated. Results of classification are tabulated in Table 1. We consider that a screening method should offer high sensitivity and pick up any abnormal cases even at the cost of false positive detections if required. Hence, we consider that 100% sensitivity is more appropriate than 100% specificity for a screening approach whereas in the case of a diagnostic method, specificity is a more important criterion than

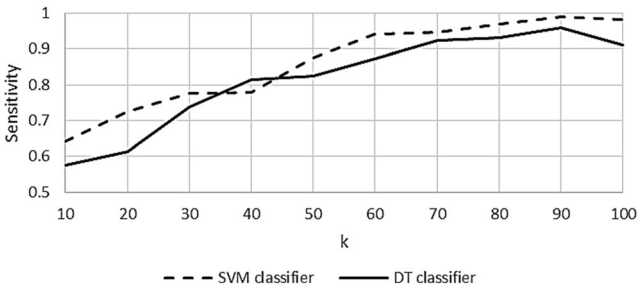

Fig. 10 Sensitivity of SVM and DT classifiers as a function of number of folds

Table 2 Average performance of SVM and DT classifiers for leave-one-out cross-validation

Classifier	Acc. (%)	Sens. (%)	Spec. (%)
SVM	98.33	98.1	98.5
DT	97.16	95	98.67

sensitivity. If we compare the sensitivities of SVM and DT classifiers as shown in Fig. 10, it can observed that the SVM classifier offers better sensitivity than the DT classifier. Hence, we select the SVM classifier for classification. It can be observed from Table 1 that for $k = 90$, sensitivity of the proposed method is 99.05% for the SVM classifier. Performance of the SVM classifier for $k = 90$ over 10 iterations is shown in Fig. 11. It can be observed from Fig. 11 that for most of the iterations, sensitivity of the classifier is 100%. Table 3 gives the summary of cervix image analysis methods in the literature. It can be observed from Table 3 that researchers have used either colposcopy images or cervicography images for development of algorithm. A clinical colposcope is not affordable in resource-poor settings. Cervicography does not provide instant decisions. A decision support system for cervical cancer screening which facilitates acquisition and processing of images with an inbuilt image processing algorithm is desirable in resource-poor settings.

This paper presents an algorithm for cervix image analysis to provide an instant decision based on images acquired through an android device. This algorithm could be packaged as a mobile application. This system of an android device loaded with analysis algorithm can act as a decision support system to provide instant decisions during cervical cancer screening in low-resource settings. Images acquired can be shown to the patient, can be sent to a distant expert for second opinion and can be stored for future references. Low cost, easy to use and handy feature make it more suitable for screening of cervical cancer in resource-poor settings. As a future work, module C of Fig. 3 is to be implemented. This report could include patient identities, images of the cervix before and after application of acetic acid and the diagnosis of decision support system.

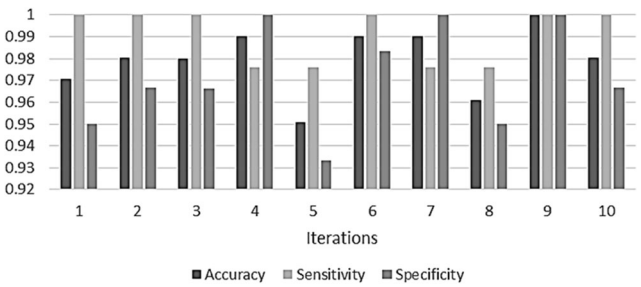

Fig. 11 Performance of SVM classifier for $k = 90$

Table 3 Summary of image analysis algorithms for cervix images

Authors	Image type	Features/classifier	Number of images	Performance
S. Y. Park et al. [16]	Colposcopy	Statistical features/KNN, SVM	29	Sensitivity 79% Specificity 88%
W. Li et al. [17]	Colposcopy	G component of RGB color space, contrast feature	99	Sensitivity 94% Specificity87%
Rama Praba et al. [18]	Colposcopy	Statistical features/Bayes	260	Sensitivity 77% Specificity 91%
Alush et al. [19]	Cervicography	Visual words/Markov random field model	211	Sensitivity 60%
Tao Xu et al. [20]	Cervicography	The pyramid histogram of oriented gradients (PHOG), the pyramid color histogram in CIE-Lab space (PLAB) and the pyramid histogram of local binary pattern (PLBP)/AdaBoost	345	Sensitivity 86.4% Specificity 74.2% Accuracy 80.3%
Sukumar et al. [21]	Cervicography	Local binary pattern, local ternary pattern and local deviation pattern/random forest classifier	280	Accuracy 95.4%
Proposed method	Android device	Color features, SGLDM features, NGTDM features, NGLDM features, wavelet features and LBP features/SVM, DT	*102*	*Sensitivity *99.05%* Specificity *97.16%* Accuracy *97.94%*

*Performance of proposed method.

Conclusions

An algorithm for image classification of digital cervix images acquired using an android device is proposed. This algorithm offers an accuracy of 97.94%, a sensitivity of 99.05% and specificity of 97.16%. This image processing algorithm can be implemented as a mobile application to be embedded in an android device. The acquired images can be analysed using this app to get instant results.

Acknowledgements We would like to acknowledge the support of Dr. Suma Nair, Associate Professor, Community Medicine Department, Kasturba Medical College, Manipal, for facilitating the acquisition of images during the screening programmes conducted.

Funding Information This publication is made possible by a subagreement from the Consortium for Affordable Medical Technologies (CAMTech) at Massachusetts General Hospital with funds provided by the generous support of the American people through the US Agency for International Development (USAID Grant number224581). The contents are the responsibility of Manipal Academy of Higher Education and do not necessarily reflect the views of Massachusetts General Hospital, USAID or the US Government.

Compliance with Ethical Standards

Conflict of Interest The authors declare that they have no conflict of interest.

Ethical Approval Institutional Ethics Committee approval was obtained for this study, and an informed consent was obtained from the women participating in the study.

References

1. Ferlay J, Soerjomataram I, Ervik M, Dikshit R, Eser S, Mathers C, Rebelo M, Parkin DM, Forman D and Bray F: GLOBOCAN 2012 v1.0, Cancer incidence and mortality worldwide: IARC Cancer Base No. 11 [Internet]. Lyon, France: IARC 2013. Available from: http://globocan.iarc.fr, accessed on 19/09/2017.
2. Sankaranarayanan R, Wesley R, Somanathan T, Dhakad N: Visual inspection of the uterine cervix after the application of acetic acid in the detection of cervical carcinoma and its precursors. Cancer 83: 2150–2156, 1998
3. Sankaranarayanan R, Shyamalakumary B, Wesley R, Sreedevi Amma N: Visual inspection with acetic acid in the early detection of cervical cancer and precursors. Int. J. Cancer 80:161–163, 1999
4. Denny L, Kuhn L, Pollack A, Wainwright H: Evaluation of alternative methods of cervical cancer screening for resource-poor settings. Cancer 89:826–833, 2000
5. Belinson JL, Pretorius RG, Zhang WH, Wu LY, Qiao YL, Elson P: Cervical cancer screening by simple visual inspection after acetic acid. Obstet Gynecol 98:441–444, 2001
6. Sangwa-Lugoma G, Mahmud S, Nasr SH, Liaras J, Kayembe PK, Tozin RR, Drouin P, Lorincz A, Ferenczy A, Franco EL: Visual inspection as a cervical cancer screening method in a primary health-care setting in Africa. Int J Cancer 119:1389–1395, 2006
7. Holger Lange: Automatic glare removal in reflectance imagery of the uterine cervix. In Proc. SPIE 5747, Medical Imaging 2005: Image Processing, San Diego, California, United States 2005, pp 2183–2192.
8. Othmane EM, Mustapha K, Hakim A, Taouq G, Yassir AB: Automatic detection and inpainting of specular reflections for colposcopic images. Cent. Eur. J. Comp. Sci. 1:341–354, 2011
9. Zimmerman-Moreno G, Greenspan H: Automatic detection of specular reflections in uterine cervical images. Proc. of SPIE Medical Imaging 6144, San Diego, California, United States, 2006, pp 2037–2045.

10. Wenjing L, Jia G, Daron F, Allen P: Automated image analysis of uterine cervical images. In Proc. SPIE Medical Imaging 6214, San Diego, California, United States 2007, pp 65142P-9P.
11. Gali Z, Shiri G, Hayit G: Automatic landmark detection in uterine cervical images for indexing in a content-retrieval system. In Proc. of IEEE International Symposium on Biomedical Imaging, Arlington, VA, USA 2006, pp 1348–1351.
12. Greenspan H, Gordon S, Zimmerman G, Lotenberg S, Jeronimo J, Antani S, Long R: Automatic detection of anatomical landmarks in uterine cervical images. IEEE Trans Med Imaging 28:454–468, 2009
13. Abhishek D, Avijit K, Debasis B: Elimination of specular reflection and identification of ROI: the first step in automated detection of cervical cancer using digital colposcopy. In Proc. 2011 I.E. International Conference on Imaging Systems and Techniques (IST), Penang, Malaysia 2011, pp 237–241.
14. Shelly L, Shiri G, Hayit G: Shape priors for segmentation of the cervix region within uterine cervical images. J. Digit. Imaging 22: 286–296, 2009
15. Lange H: Automatic detection of multi-level acetowhite regions in RGB color images of the uterine cervix. In Proc. of SPIE Medical Imaging 5747, San Diego, California, United States 2005, pp 1004–1017.
16. Park SY, Follen M, Milbourne A, Rhodes H, Malpica A, MacKinnon N, MacAulay C, Markey MK, Richards-Kortum R: Automated image analysis of digital colposcopy for the detection of cervical neoplasia. J. Biomed. Opt 13:014029, 2008
17. Li W, Venkataraman S, Gustafsson U, Oyama JC, Ferris DG, Lieberman RW: Using acetowhite opacity index for detecting cervical intraepithelial neoplasia. J. Biomed. Opt 14:014020, 2009
18. Rama Praba PS, Ranganathan H: Computerized lesion detection in colposcopy cervical images based on statistical features using Bayes classifier. In Proc. of the InConINDIA, AISC 132, Visakhapatnam, India 2012, pp 597–604.
19. Alush A, Greenspan H, Goldberger J: Automated and interactive lesion detection and segmentation in uterine cervical images. IEEE Trans Med Imaging 29:488–501, 2010
20. Xu T, Kim E, Huang X: Adjustable adaboost classifier and pyramid features for image-based cervical cancer diagnosis. In Proc. International Symposium on Biomedical Imaging (ISBI), New York, NY, USA 2015, pp 281–285.
21. Sukumar P, Gnanamurthy RK: Computer aided screening of cervical cancer using random forest classifier. RJPBCS 7:1521–1529, 2016
22. Ji Q, Engel J, Craine E: Texture analysis for classification of cervix lesions. IEEE Trans Med Imaging 19:1144–1149, 2000
23. Yeshwanth S, Brian N, Sunanda M, Sonal B: A unified model-based image analysis framework for automated detection of precancerous lesions in digitized uterine cervical images. IEEE J Select Top Signal Process 3:101–111, 2009
24. Park SY, Sargent D, Liebeman R, Gustafsson U: Domain-specific image analysis for cervical neoplasia detection based on conditional random fields. IEEE Trans Med Imaging 30:867–878, 2011
25. Zhiyun X, Rodney LL, Sameer A, George RT: Automatic extraction of mosaic patterns in uterine cervical images. Computer-Based Medical Systems (CBMS) 2010 I.E. 23rd International Symposium, Perth, WA, 2000, pp 273–278.
26. Song D, Edward K, Xiaolei H, Joseph P, Hctor MA, Je H: Multimodal entity coreference for cervical dysplasia diagnosis. IEEE Trans Med Imaging 34:229–245, 2015
27. Quinley KE, Gormley RH, Ratclie SJ, Shih T, Szep Z, Steiner A, Ramogola-Masire D, Kovarik CL: Use of mobile telemedicine for cervical cancer screening. J Telemed Telecare 17:203–209, 2011
28. Catarino R, Vassilakos P, Scaringella S, Undurraga-Malinverno M, Meyer-Hamme U, Ricard-Gauthier D, Matute JC, Petignat P: Smartphone use for cervical cancer screening in low-resource countries: a pilot study conducted in Madagascar. PLoS ONE 10:1–10, 2015
29. Ricard-Gauthier D, Wisniak A, Catarino R, van Rossum AF, Meyer-Hamme U, Negulescu R, Scaringella S, Jinoro J, Vassilakos P, Petignat P: Use of smartphones as adjuvant tools for cervical cancer screening in low-resource settings. J Lower Genit Tract Dis 19:295–300, 2015
30. Rashmi B, Vanita S, Radhika S, Niranjan K, Payal K, Sarif KN, Vidya C, Lovi G, Soubhik P: Feasibility of using mobile smartphone camera as an imaging device for screening of cervical cancer in a low-resource setting. J Postgrad Med Edu Res 50:69–74, 2016
31. Kudva V, Prasad K, Guruvare S: Detection of specular reflection and segmentation of cervix region in uterine cervix images for cervical cancer screening. IRBM 38:218–291, 2017
32. Claude I, Pouletaut P: Integrated color and texture tools for colposcopic image segmentation. In Proc. IEEE International Conference on Image Processing, Thessaloniki, Greece 2001, pp 311–314.
33. Haralick RM, Shanmugan K, Dinstein I: Textural features for image classification. IEEE Trans. Syst., Man, Cybern, SMC 3: 610–621, 1973
34. Amadasun M, King R: Textural features corresponding to textural properties. IEEE Trans. Syst., Man, Cybern 19:1264–1274, 1989
35. Sun C, Wee WG: Neighbouring gray level dependence matrix. Comput. Vision, Graphics Image Processing 23:341–352, 1982
36. Ojala T, Pietikainen M, Maenpaa T: Multiresolution gray scale and rotation invariant texture classification with local binary patterns. IEEE Trans. Pattern Anal. Mach. Intell. 24:971–987, 2002
37. Jouni P, Okko R, Serdar K: Feature selection methods and their combinations in high-dimensional classification of speaker likability, intelligibility and personality traits. Comput Speech Lang. 29: 145–171, 2015
38. Ross Quinlan J: Induction of decision trees. Machine Learning 1: 81–106, 1986
39. Torre LA, Bray F, Siegel RL, Ferlay J, Lortet-Tieulent J, Jemal A: Global cancer statistics, 2012. CA Cancer J Clin. 65:87–108, 2015
40. Mishra GA, Pimple SA, Shastri SS: An overview of prevention and early detection of cervical cancers. Indian J. Med. Paediatr. Oncol 32:125–132, 2011